A synoptic view of X-ray in-flight calibration plans[1]

Matteo Guainazzi[a,b], Laurence David[c], Catherine Grant[d], Jukka Nevalainen[e], Marc Audard[f]

[a]ESA-European Space Astronomy Centre (ESAC), Villafranca del Castillo, E-28692, Madrid, Spain

[b]Institute of Space and Astronautical Science, Japan Aerospace Exploration Agency (JAXA), 3-1-1 Yoshinodai, Chuo-ku, Sagamihara, Kanagawa 252-5210, Japan

[c]Harvard-Smithsonian Center for Astrophysics, 60 Garden St., Cambridge, MA 02138, USA

[d]Massachusetts Institute of Technology 37-551, 77 Massachusetts Ave., Cambridge, MA 02139-4307

[e]Tartu Observatory, 61602 Toravere, Estonia

[f]Department of Astronomy, University of Geneva, Ch. d'Ecogia 16, 1290, Versoix, Switzerland

Abstract. Ideally a complete set of ground-based calibration measurements should under-pin a full characterization of the physical model describing detectors flown on-board space observatory. More often then not, however, this is not the case due to time and budgetary restrictions during the development phase, or to the - somewhat inevitable and unpredictable - degradation of instrument performance in space. In this paper we present a synoptic view of the set of celestial sources used for in-flight calibration of X-ray detectors by past and operational missions. This summary could be beneficial for future mission to optimize the critical early phases of their science operations.

Keywords: X-ray instrumentation - Operations - X-Rays:general.

Address all correspondence to: Matteo Guainazzi; E-mail: Matteo.Guainazzi@sciops.esa.int

1 The art of calibrating X-ray instruments

Ideally, calibration of space X-ray instruments is the result of a complete physical model supported by an adequate set of ground-based measurements under controlled conditions. Regrettably, time and budget pressure during the mission development phase, as well as the degradation of the instrument performance in space (radiation damage, contamination, electronic failures, degrading thermal environment) more often than not require re-calibration using celestial sources. "In-flight" calibration programs have been playing a crucial role in our understanding of the instrument scientific performance, as well as (and, often, more crucially) of their time evolution.

While X-ray astronomy is nowadays a fully mature and globally integrated science, calibration of X-ray space instruments was carried out for decades in isolation, and with little cross-talk among

---

[1]This paper was written in the framework of the activities of the IACHEC Heritage Working Group

calibration teams of different instruments and know-how transfer from older to newer mission (besides the natural transfer of calibration scientists to newer projects). This has led to a wide variety of approaches in dealing with similar calibration issues over different missions, as well as to a surprisingly large variety of celestial sources being used for the same calibration purpose. Moreover, the suitability of a celestial source for calibration purposes depends on the commensurability between observables related to the intrinsic astrophysical properties and instrument performance. For instance, thermal or velocity broadening of emission line profiles have got a negligible impact on the calibration or energy scale and line spread function at CCD resolution ($\Delta E/E \sim 10$), while they should be taken into account at grating or calorimeter resolution ($\Delta E/E / approx gt 100$).

The birth of the *International Astronomical Consortium for High-Energy Calibration* (IACHEC; `http://web.mit.edu/iachec/`)[1] in 2006 tried to alleviate this original sin, by achieving a better integration among calibration activities of operational high-energy observatories. In this context the IACHEC aims to provide standards for high energy calibration and supervise cross calibration between different missions. This goal is reached through working groups, where IACHEC members cooperate to define calibration standards and procedures. The scope of these groups is primarily a practical one: a set of data and results (eventually published on refereed journals) will be the outcome of a coordinated and standardized analysis of reference sources ("high-energy standard candles"). Past, present and future high-energy missions can use these results as a calibration reference. In this context one of the goals of IACHEC is to develop a web-based archive of calibrated data sets and response files for all "standard candles" from all high energy missions. This suite of calibrated data sets can then be used to ensure a proper cross-calibration. Imprinted in the genetic code of the IACHEC is also the goal of providing future missions with a test-bed of consolidated experiences and good practices, that can be beneficial in designing and optimizing

2

in-flight calibration plans.

Regrettably, calibration of X-ray astronomy instrumentation cannot rely on "standard candles" *stricto sensu*, *i.e.* on sources whose absolute flux is known once other astrophysical observables are measured. One must be content with sources for which an educated guess of the physical process responsible for their X-ray emission is available. These "X-ray standard candles" exhibit non-thermal broad-band spectra, or thermal spectra in the soft X-ray band. For each source in this set of "X-ray standard candles", the IACHEC aims to define data reduction and analysis procedures, and a reference astrophysical model; and to publish these, ideally in refereed journals.

In this paper we review the in-flight calibration plans of all the missions active in the IACHEC context (basically, all the operational X-ray observatories from the 90s of the past century to now). Our primary goal is providing a synoptic view of in-flight calibration programs of past and operational X-ray space missions that might be used by future missions to optimize the preparation of their calibration operations after launch.

In Appendix A we list the instruments discussed in this paper.

2 High-resolution LSF and wavelength scale

Spectra of X-ray bright cool stars have been used for the calibration of the Line Spread Function and wavelength scale in the *Chandra*/LETG and HETG and the XMM-Newton/RGS (Tab. 1): ABDor, Algol, Capella, HR1099, and Procyon[2] (Fig. 1). Capella is on the average the brightest, and the least variable in this sample: its historical RGS light curve exhibits a dynamical range of $\pm15\%$ (Andy Pollock, private communication). ABDor and HR1099 exhibit large flaring activities, with flux changes of up to one order of magnitude on time scales as short as few hours.[3,4]
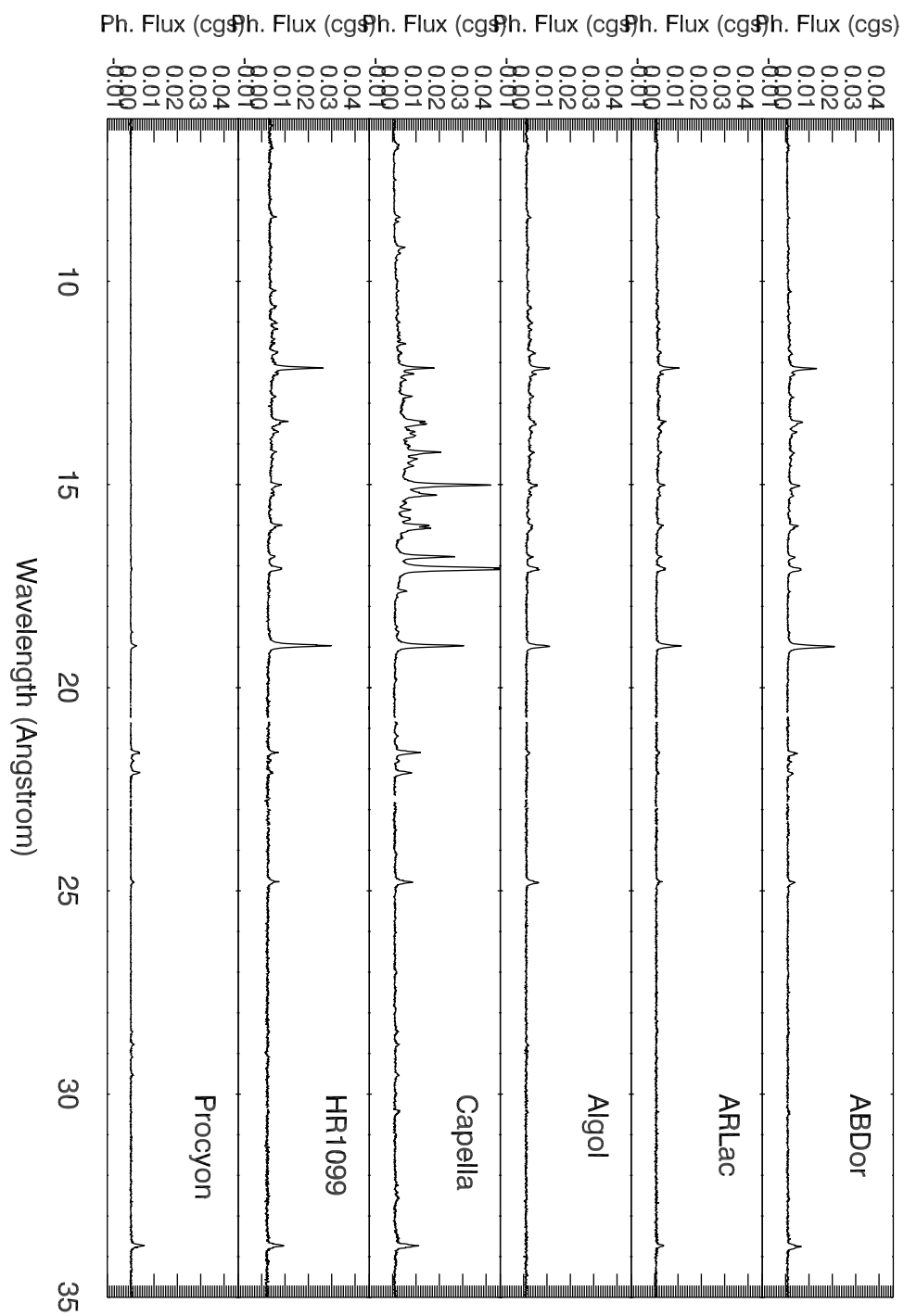
Fig 1 RGS spectra from the longest XMM-Newton observation of five cool stars used for the calibration of the LSF and wavelength scale. The spectra are displayed in on the same linear scale on the y-axis to ease comparison.

Table 1 Main sources used for the calibration of the LSF and wavelength scale in high-resolution detectors

Source	LETG	HETG	RGS
Capella	X	X	X
HR1099		X	X
Procyon	X		X

The spectrum of some of these stars (Capella, most notably) is too soft to cover adequately the whole X-ray spectral bandpass. This is particularly important for the future calibration of the micro-calorimeter on-board Astro-H at the astrophysically crucial iron atomic transitions at 6–7 keV. HR1099 and ABDor are sufficiently hot for this purpose, once the thermal broadening of emission lines is taken into account. Fe-K fluorescence lines are commonly observed, for instance, in the spectra of X-ray Binaries (XRB). A population of heavily obscured XRBs, whose Fe line exhibits a very large (keV) Equivalent Width (EW) exists. Among the best-studied (and brightest) examples of this sample are IGRJ16318+4848,[5] and GX301-2.[6] Their lines are unresolved at the Chandra/HETG resolution. However, curve-of-growth analysis, and other considerations are compatible with these lines being produced in the wind of the OB companion.[7] The Chandra upper limit on the width is 770 km/s, while the value stemming from terminal velocity of the star wind is 850 km/s. More worryingly, lines produced in stellar wind may have a complex structure, with red wings.[8] For these reasons, these sources could be considered for calibration of micro-calorimeter detectors at 6 keV only after observations with ASTRO-H would provide better astrophysical clues as to their origin and intrinsic profiles.

Table 2 Main sources used for the calibration of CTI, gain, and redistribution in CCD X-ray detectors

Source	ACIS	EPIC-MOS	EPIC-pn	XIS	XRT
1E0102-72	X	X	X		X
3C273		X			X
CasA	X	X	X		X
Cygnus Loop				X	
Perseus Cluster		X		X	
PKS2155-304		X			X
RXJ1856.5-3754		X			X
Tycho SNR		X	X		X
Vela SNR			X		
ζPuppis		X	X		
ζOrionis		X	X		

3 CCD redistribution, resolution and energy scale

While the redistribution shape can be in principle adequately characterized by illuminating the cameras with monochromatic beams on ground, spectral degradation induced by various form of radiation damage required a re-calibration of the photon redistribution alongside the energy scale (Charge Transfer Inefficiency, CTI, and gain) in several X-ray space Charge Couple Devices (CCD). A list of the main targets used for this purpose is given in Tab. 2. Point-like sources bright enough to produce sufficient counts cannot be used by the *Chandra*/ACIS due to pile-up. Characterization of the CTI requires uniform illumination of the whole CCD with a source of known spectra, ideally with well isolated (at CCD resolution) atomic transitions. In the XMM-Newton/EPIC cameras a specific position of the filter wheel (CAL_CLOSED) let a ^{55}Fe source shine through the whole field-of-view. Similarly, a ^{55}Fe source is shone onto the ACIS field-of-view when it is transferred into the stowed position before and after each passage through the radiation belts. The ^{55}Fe source has a life time of only 2.7 years. This is a potential issue for long

missions such as *Chandra* or XMM-Newton. The decreasing source flux, the different illumination conditions when compared with typical astronomical background, and the limited spectral range where the ^{55}Fe produces atomic transitions requires complementing these measurements with observations of extended sources with strong and well isolated (at CCD resolution) atomic transitions. The Vela Supernova Remnant (SNR) covers the whole $\simeq$30' side EPIC field-of-view, and it has been extensively used by the EPIC calibration team to calibrate the readout losses. Strong galaxy clusters such as Centaurus or Perseus have corroborated the calibration results. The *Suzaku*/XIS and the Swift/XRT also make use of ^{55}Fe calibration sources which permanently illuminate small regions of the CCDs. Large scale sources such as the Cygnus Loop ($\simeq$3°), Puppis A (50'×60'), or observations of the bright Earth have been used by XIS for CTI measurements. The characterization of transfer losses in the central area of the XRT made use of compact X-ray bright SNR such as Cas A, IC443, or Tycho. Tycho is also one of the targets used to characterize transfer losses in the EPIC-MOS. A compilation of EPIC-MOS images of SNRs is shown in Fig. 2 showing examples of compact (<2'), intermediate ($\simeq$5'), and large ($\gtrsim$30') sources used for calibration purposes.

The study of spectral degradation in space also requires bright sources with well isolated (at CCD resolution) atomic transitions. Cassiopeia A was the official first-light target for Chandra, primarily because it is bright, has many well-separated spectral features, and is matched in size to an ACIS CCD. The most used and studied source in the IACHEC context is, however, the compact ($\simeq$1' diameter) SNR 1E0102-72.3.[9] The combination of symmetric morphology, lack of Fe lines, strong and well isolated OVII, OVII, NeIX, and NeX emission lines, detailed empirical and astrophysical modeling, and deep available observations with all major operational CCD in space (together with a flux constant at a level of better than 1% in all knots; Frank Haberl, private communication) make of 1E0102-72.3 a widely used "standard candle" in soft X-ray astronomy.[10] Stars
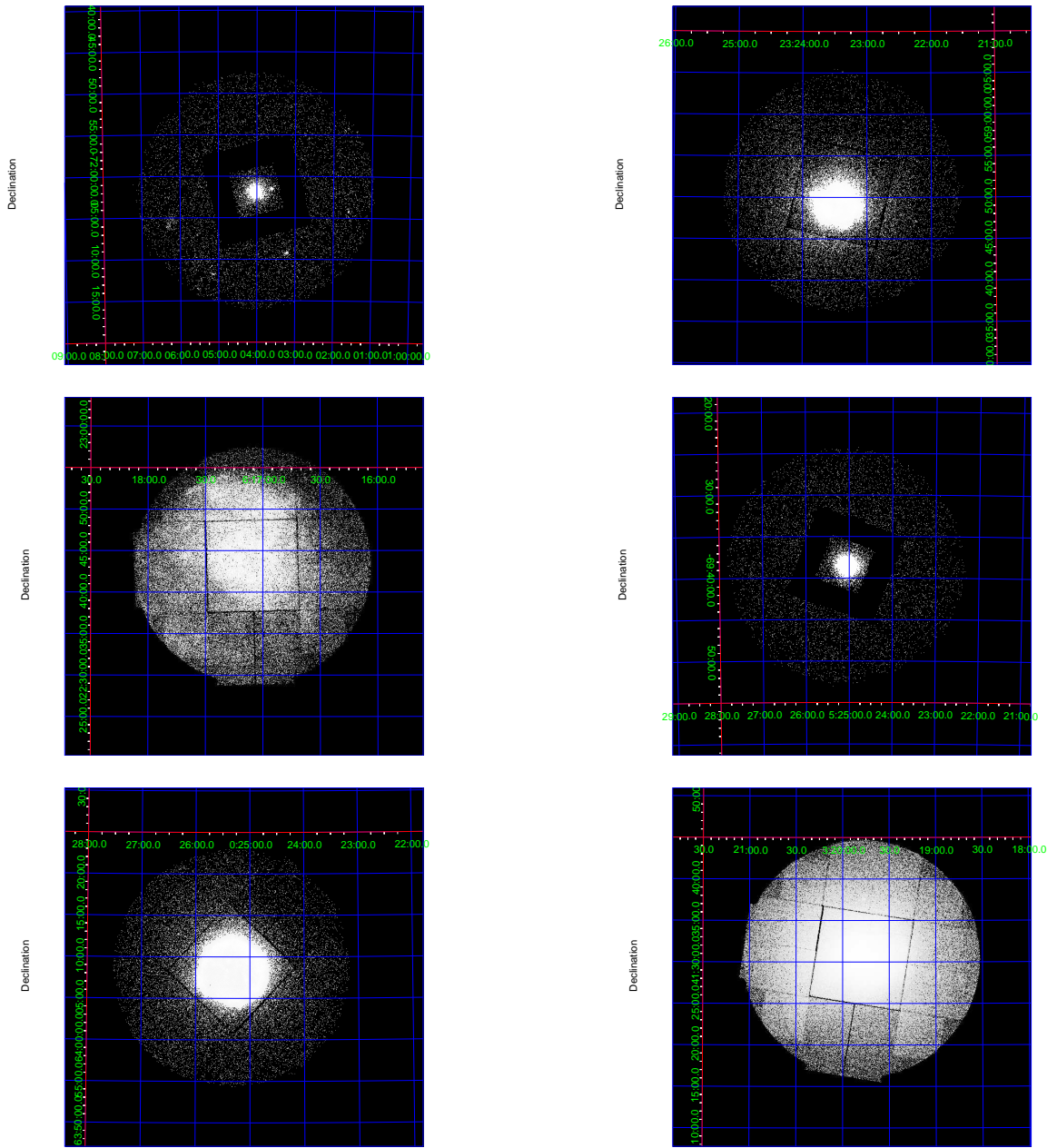
Fig 2 EPIC-MOS2 image of the deepest XMM-Newton observation of five SNR and one galaxy cluster used for calibration of the energy scale and redistribution in X-ray astronomy CCD detectors. *From top left to bottom right*, 1E0102-72, CasA, IC443, N132, Tycho, and the Perseus galaxy cluster. The EPIC-MOS field of view is about 30'×30'.
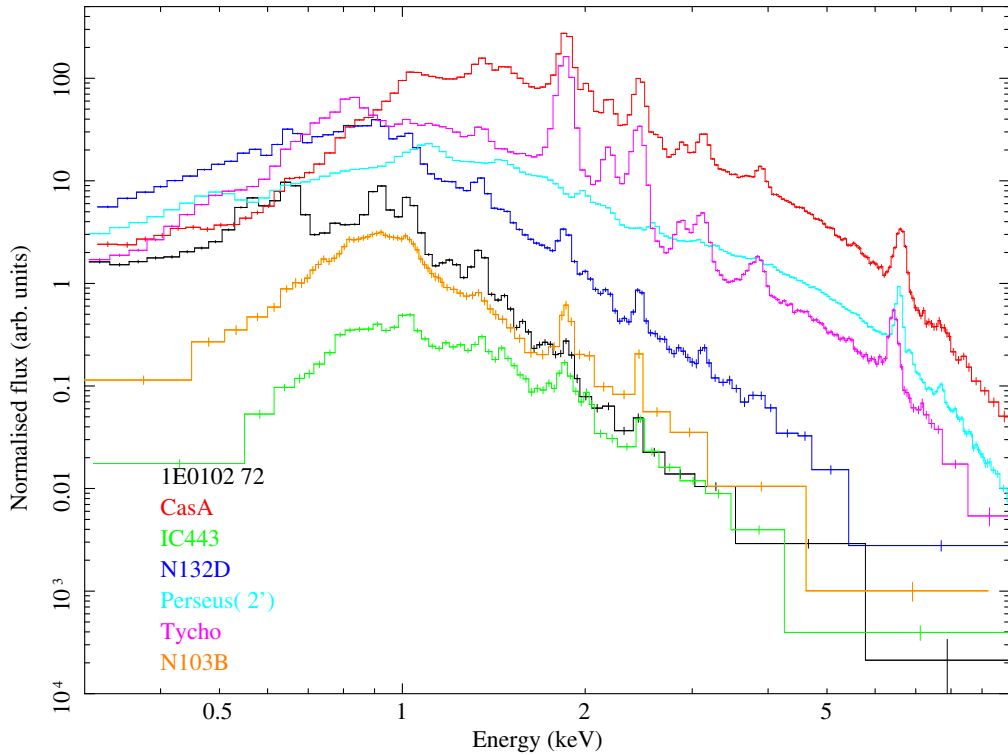
Fig 3 EPIC-MOS1 spectra of SNR and galaxy clusters used for CCD redistribution calibration

like ζPuppis and ζOrionis offer alternatively strong NV lines. Very soft continuum sources such as the isolated neutron stars RXJ0720.4-32.5 or RXJ1856.6-3754 offer complementary information thanks to their simple blackbody-like spectrum,[11] and - at least for the latter source - extreme stability.[12] Additional calibration of the redistribution can be achieved by looking at the agreement between data and models in bright power-law sources at energy ranges where the effective area exhibits the steepest gradients. GBH binaries such as LMCX-3, or radio-loud AGN such as 3C273 and PKS2155-304 have been used for this purpose. These same sources have also been used by ACIS to calibrate the energy scale at low energies (¡ 500 eV) using gratings observations.

Finally, it is possible to use heavily obscuring sources to constrain the redistribution shelves. This is a particularly promising approach for CCD "Fast Modes" (EPIC-pn Timing and Burst

9

Mode, XRT Window Timing Mode, or the Continuous Clocking Mode in ACIS). Extremely bright obscured binaries can in principle provide an almost uncontaminated view of photons redistributed below 2 keV. The main astrophysical issue is disentangling possible sources of soft excess such as dust-halo scattering, or coronal emission.

4 Area at energies <10 keV

In optical astronomy, there are many stable point sources (mostly stars) with a range of colors that can be used as standard candles. While there are stable point sources in the soft X-ray band ($\lesssim$1 keV; e.g., white dwarfs and isolated neutron stars), there are no stable point sources in the medium X-ray band (1–10 keV; also conventionally referred to as the "hard X-ray CCD band). For this reason, extended sources (e.g., supernova remnants and clusters of galaxies) are commonly used as standard candles in the hard X-ray band. In addition, only faint point sources can be used to prevent pile-up effects in CCDs and gratings observations of extended sources are excluded to prevent degradation in the spectral resolution.

4.1 Point-like sources

Given the intrinsic correlation between redistribution and effective area calibration of CCDs in the soft energy band, the most commonly used sources for the in-flight calibration of the soft X-ray effective area are largely coincident with those used for the calibration of the redistribution (Tab. 3). Compact SNR (1E0102-72.3), active stars with well isolated He-like and H-like emission line complexes (ζPuppis; ζOrionis), and very soft Isolate Neutron Starts (INS; RXJ1856.6-3754). In the EUV/extreme soft X-ray band, White Dwarfs such as Sirius B, GD153 or HZ43 have been used to create empirical adjustments to the effective area.

Table 3 Main sources used for the calibration of the effective area below 10 keV

Source	HRC	LETG	HETG	RGS	ACIS	EPIC-MOS	EPIC-pn	GSC	SSC	JEM-X	PCA	XIS	XRT
1E0102-72					X	X						X	X
3C273		X	X										X
Abell1795					X	X	X					X	X
Abell2029					X	X	X						X
Coma cluster						X	X						
Crab Nebula				X				X	X	X	X		X
G21.5-0.9	X				X								X
H1426+428			X										X
HZ43	X	X											
Mkn421	X	X	X	X									X
Perseus Cluster						X	X						
PKS2155-304	X	X	X	X								X	
RXJ1856.5-3754		X		X								X	X

In the hard CCD-band, radio-loud AGN such as 3C273, H1426+128, and PKS2155-304 are still widely used for effective area calibration. A cross-calibration campaign on PKS2155-304 (now involving *Chandra*, NuSTAR, *Suzaku*, *Swift*, and XMM-Newton) has been running continuously since 2006,[13] with one observation every year. However, radio-loud AGN, and in particular blazars (Mkn421, PKS2155-304) are rapidly variable sources, with a complex flux-dependent spectral variability. *Chandra* and XMM-Newton CCD observations of these objects are almost invariably affected by pile-up. For this reason, *Chandra* observes Mkn421 and PKS2155-304 only with the gratings. Mitigation actions in the latter case involve excising the PSF core from the spectral accumulation region, yielding additional uncertainties in the spectral de-convolution due to the Encircled Energy Fraction of the PSF wings.[14] The usage of serendipitous catalogs for effective area calibration and cross-calibration has been proposed as a possible alternative.[15, 16]

Plerionic spectra may represent a promising alternative (besides the Crab, still used for the cali-

bration of the RXTE/PCA, the NuSTAR instruments, and the instruments on-board MAXI, among others). The IACHEC study on G21.5-0.9[17] is currently the largest published cross-calibration study ever in terms of number of instruments involved, covering the whole energy band from 2 to 150 keV (the source is obscured by a column density $\simeq 2 \times 10^{22}$ cm^{-2}).

4.2 On galaxy clusters as calibration sources

Galaxy clusters have been extensively used as calibration sources because they are stable on human time-scales. This implies that the same cluster can be used at any time for any hard X-ray detector calibration observation, and compared with observations taken in other epochs by the same or other detectors. The nearest clusters hotter than about 6 keV are bright and hard, thus yielding sufficient photons for calibration experiments within typical standard X-ray calibration experiments' duration (a few hours). However, due to their surface brightness distribution they are not too bright to produce pile-up in CCD detectors. The combination of these factors makes of galaxy clusters very suitable targets for effective area shape calibration, above 2 keV as well as in the 0.5-1.0 keV energy band.[18–20] Large cluster samples can be formed for calibration or cross-calibration purposes (see, *e.g.*, Schellenberger et al. 2015). The only significant line emission in clusters hotter than 6 eV is due to recombination transitions from FeXXV and FeXXVI. The energy band covered by these these lines ($\simeq 6.67$ to 6.96 keV) is narrow. The dependence of the effective area on energy in this energy range is smooth and shallow. This allows to decouple energy redistribution and effective area calibration effects. However, the extended nature of the X-ray emission in clusters is at the same time a curse and a blessing. It causes different sensible sky areas being covered in different detectors. This requires additional exposure map corrections, known with different degrees of uncertainties in different detectors.

12

Relaxed galaxy clusters such as Abell 1795 have been also extensively used.[19] Abell 1795 has been used to monitor the spatial distribution of the contaminant in ACIS. At the same time, galaxy clusters have assumed the role of reference "standard candles" in the hard X-ray band, following the pioneer cross-calibration work by Nevalainen et al. (2010). These authors found that the gas temperature in clusters of galaxies derived from the 2-6 keV continuum emission is in good agreement with that derived from the H- to He-like Fe line ratio for the EPIC cameras (see, *e.g.*, Fig.10 in Nevalainen et al. 2010). This method requires a very large number of photons in the narrow range, and has encountered so far limited application with real data, due to the very deep exposures needed. It opens, however, promising perspectives for future high-resolution detectors at the Fe transition energies, such as the micro-calorimeters on board ASTRO-H.

Thanks to their flux stability, simple and well understood physics galaxy clusters are excellent calibrator candidates for the high-resolution instrument on-board ASTRO-H (Soft X-ray Spectrometer, SXS[21]). The ideal source should have the best combination of X-ray flux, small cool core (in order to ensure the largest possible isothermal area), and extension. These quantities are shown in Fig. 4 for the 11 objects of the Nevalainen et al. (2010) sample (see also Sect. 8).

5 Area at energies >10 keV

Most of the operational instruments above 10 keV have employed the Crab Nebula as primary calibrator for the effective area. The response of the RXTE/PCA[22] and NuSTAR has been calibrated solely based on the Crab, assuming "standard values" for the photon index and normalization of a power-law shape. Weisskopf et al. (2010) showed that some models of the nebula high-energy emission predict a spectral curvature, that should be already measurable by the PCA. This evidence challenges the assumption underlying the calibration of its response. The status of the Crab Neb-
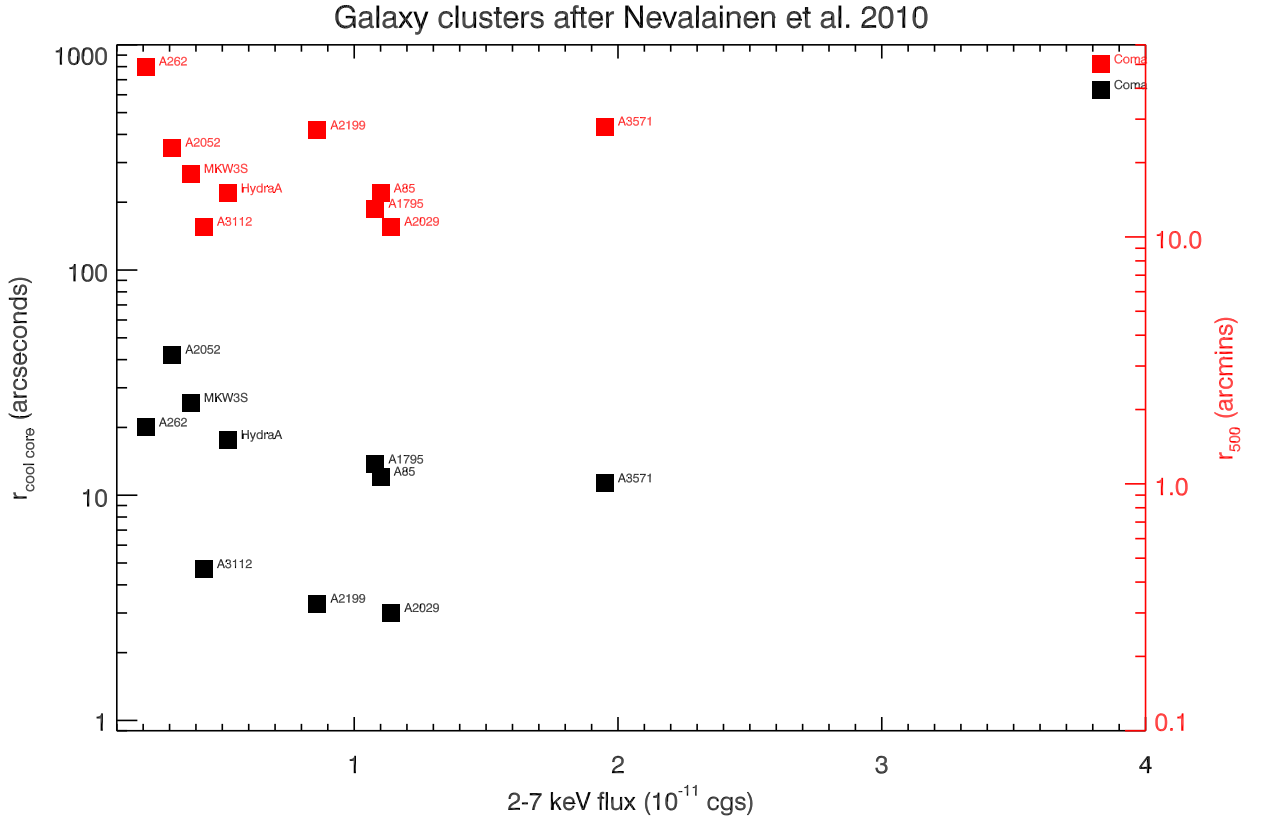
Fig 4 Radius of the cool core ($r_{coolcore}$, *black squares*, *left y-axis*), and r_{500} (*red squares*, *right y-axis*) as a function of the 2–7 keV flux for the sample of galaxy cluster after Nevalainen et al. (2010)

ula as "the standard candle of X-ray astronomy" has been severely undermined, however, by two circumstances: a) the fact that most instruments operating below 10 keV during the first decade of the XXI century could not observe the Crab due to telemetry or pile-up limits, except in special, rarely used instrumental modes; b) the discovery that the Crab is actually a variable source[23] exhibiting variations with a dynamical range of $\simeq$7% over the whole X-ray band on time-scales of months (a discovery delayed by the assumption that the Crab Nebula was a stable calibration source!). Alternative plerionic spectra such as G21.5-0.9 and MSH15-52 could yield a statistical accuracy on the determination of the spectra shape of $\Delta\Gamma \sim 0.05$ in a 50 ks observation with the hard X-ray focusing telescopes on NuSTAR and Astro-H. With a NuSTAR observation of 280 ks

Table 4 Sources used for the calibration of the effective area above 10 keV

Source	AGILE	BAT	HXD	HEXTE	IBIS	NuSTAR	SPI
Crab Nebula	X[a]	X	X	X	X	X	X
PSR1509-58			X		X		

[a]Crab pulsar

of G21.5-0.9, the error on the spectral index ($\Delta\Gamma\simeq0.013$) is comparable to the systematic error due to uncertainties in the effective area calculations (K.Madsen, private communication). These performances are comparable to those of a bright radio-loud hard AGN such as 3C273[24] or Centaurus A.[25] However, 3C273 exhibit a hard X-ray flux historical variability of about 50%.[24] Typical observed spectra for the sources discussed in this Section are shown in Fig. 5.

6 PSF

"First-light"-like bright sources such as X-ray binaries (CygX-1, CygX-2, HerX-1), stars (AR Lac, Capella) or bright AGN (3C273, MCG-6-30-15) have been used for this purpose, depending on the brightness limitations.

Since ACIS observations of bright point sources produce significant pile-up, the Chandra team has generated a composite on-axis PSF from HRC-I observations of Ar Lac and Capella and an ACIS observation of Her X-1.[30–32] The Ar Lac and Capella data are used to measure the inner and outer core of the on-axis PSF, respectively, while the ACIS observation of Her X-1 (which is heavily piled-up) is used to measure the wings of the PSF. Her X-1 is a bright point source with a low column density and no dust halo. These three observations are re-normalized to produce the on-axis PSF from 0.5" to 10'. Both the on-axis and off-axis PSF are measured and monitored by yearly HRC-I raster scans of AR Lac.
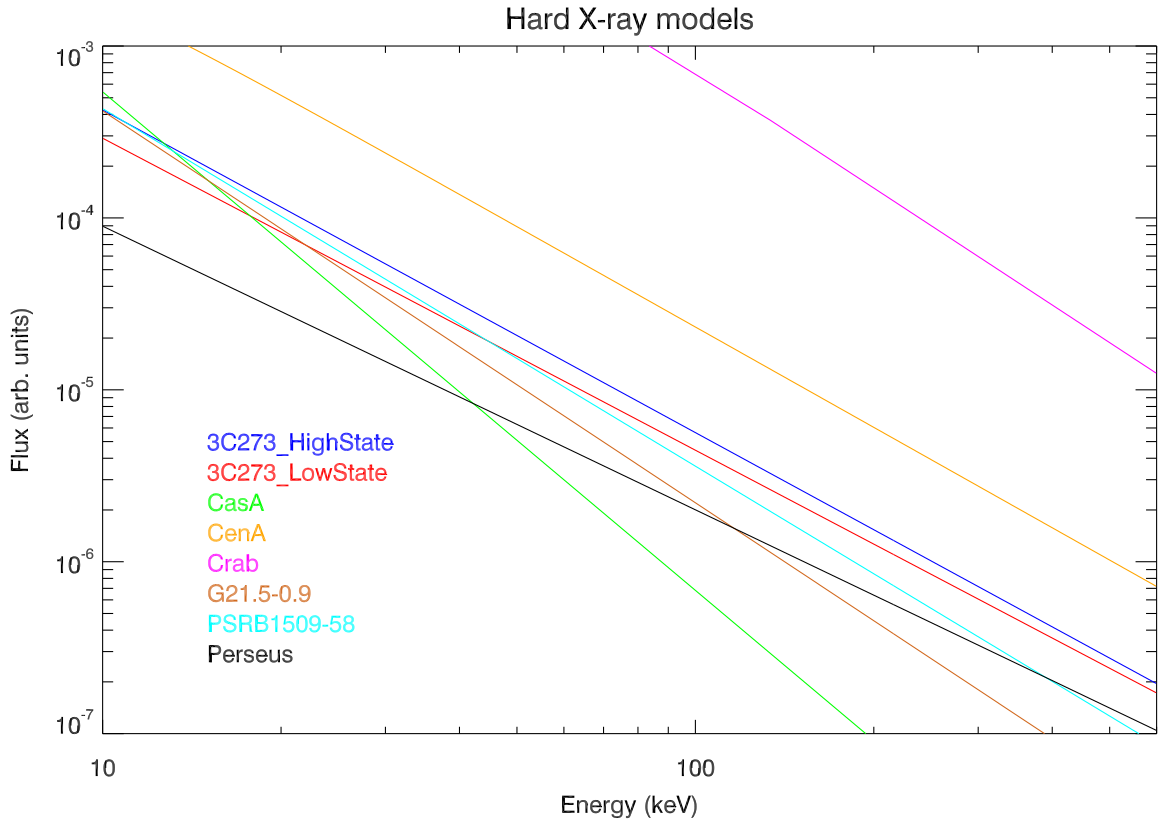
Fig 5 Models of plerionic spectra above 10 keV: Crab (*black*);[26] G21.5-0.9 (*red*);[17] PSR1509-58 (*green*).[27] They are compared to the spectra of the SNR Cas A (*blue*)[28]), and 3C273 in its lowest (*cyan*) and highest (*magenta*) state in the 2003–2005 INTEGRAL and XMM-Newton monitoring.[29] The numbers in *brackets* indicate the 90% confidence level error on the photon index (one interesting parameter).

7 Timing

The Crab pulsar ($\simeq$33 ms) has been the main target used for timing calibration.[33,34] Alternative targets have been: A0535-262 (103 s), AE Aqr (33 s), Am Her (11140 s), Her X-1 (1.237 s), PSR B0540-69 (51 ms) PSR J0537-69 (50 ms), PSR B1055-52 (197 ms), PSR B1509-58 (in MSH15-52; 0.15135 s), Vela pulsar (88 ms)

8 Cross-calibration

Several IACHEC Working Groups[†] have been engaged in defining "standard candle" for cross-calibration purposes:

- **Clusters of Galaxies**: Nevalainen et al. (2010) discuss a sample of bright clusters of galaxies, used for the verification of the cross-calibration status among the operational CCD cameras in the 0.7–10 keV energy band, as well as for the re-calibration of the *Chandra* effective area embedded in the CALDB change between 3.4 and 4.1. The sample is constituted by: Abell 1795, Abell 2029, Abell 2052, Abell 2199, Abell 262, Abell 3112, Abell 3571, Abell 85, Coma, HydraA, MKW3S.

- **Effective area**: This WG has been running a cross-calibration campaign on PKS2155-304 since 2006.[13] This campaign is constituted by simultaneous observations of with *Chandra*, NuSTAR, *Suzaku*, Swift, and XMM-Newton. Other blazars such as 3C273 and H1426+428 are the basis of a systematic comparison of the effective area calibration between the *Chandra* gratings and the XMM-Newton X-ray payload (Smith & Marshall, in preparation)

[†]`http://web.mit.edu/iachec/wgs`

- **Non-thermal SNR**: This WG deals primarily with effective area cross-calibration above 10 keV. The pioneer work by[35] on the Crab Nebula, has been later challenged.[23,36] An update of this study, solely based on quasi-simultaneous observations, is being published (Natalucci et al., in preparation). Alternative, albeit weaker, plerionic spectra have been proposed for this purpose, such as G21.5-0.9.[17]

- **Thermal SNR**: The compact SNR 1E0102-72.3 has become a standard calibration target for redistribution and effective area monitoring. A semi-empirical model based on a continuum version of the APEC code[37] was developed to describe its soft X-ray spectrum, and constrained observationally using the RGS spectra. The 1E0102-72.3 spectra are used to constrain the cross-calibration of the effective area at the energy of strong and well-isolated (at CCD resolution) He- and H-like transitions of OVII, OVIII, NeIX, and NeX[10]

- **White Dwarfs and Isolated Neutron Stars**: The main goal of this WG is the refinement of the LETGS effective area in the softest X-ray energy band (λ>40). Sources used for this purpose are WDs such as GD153, Hz43, and Sirius B, as well as the INS RXJ1856-6-3754.

List of instruments discussed in this paper

- AGILE: Astro-rivelatore Gamma a Immagini LEggero (AGILE)

- *Chandra*: Advanced CCD Imaging Spectrometer (ACIS), Low Energy Transmission Grating (LETG), High Energy Transmission Grating (HETG), High Resolution Camera (HRC)

- Integral: Imager on Board the Integral Satellite (IBIS), Spectrometer on Integral (SPI), Joint European X-ray Monitor (JEM-X)

- <u>MAXI</u>: Gas Slit Camera (GSC), Solid-state Slit Camera (SSC)

- <u>NuSTAR</u>: Nuclear Spetroscopy Telescope ARray (NuSTAR)

- <u>RXTE</u>:High-Energy X-ray Timing Experiment (HEXTE), Proportional Counter Array (PCA)

- *Suzaku*: Hard X-ray Detector (HXD), X-ray Imaging Spectrometer (XIS)

- *Swift*: Burst Alert Telescope (BAT), X-Ray Telescope (XRT)

- XMM-*Newton*: European Photon Imaging Camera (EPIC), Reflection Grating Spectrometer (RGS)

References

1 S. Sembay, M. Guainazzi, P. Plucinsky, and J. Nevalainen, "Defining high-energy calibration standards: IACHEC (International Astronomical Consortium for High-Energy Calibration)," *AIPC* **1248**, 193 (2010).

2 J.-U. Ness, J. Schmitt, V. Burwitz, R. Mewe, A. Raassen, R. van der Meer, P. Predehl, and A. C. Brinkman, "Coronal density diagnostics with Helium-like triplets: CHANDRA-LETGS observations of Algol, Capella, Procyon, epsilon Eri, alpha Cen A&B, UX Ari, AD Leo, YY Gem, and HR 1099," *A&A* **394**, 911 (2002).

3 M. Audard, M. Güdel, J. Drake, and V. Kashyap, "Extreme-ultraviolet flare activity in late-type stars," *ApJ* **541**, 396 (2000).

4 S. S. Lalitha and J. Schmitt, "X-ray activity cycle on the active ultra-fast rotator AB doradus A. implication of correlated coronal and photometric variability," *A&A* **559**, 119 (2013).

5 L. Barragán, J. Wilms, K. Pottschmidt, M. Nowak, I. Kreykenbohm, R. Walter, and J. Tomsick, "Suzaku observation of IGR J16318-4848," *A&A* **508**, 1275 (2009).

6 F. Fürst, S. Suchy, I.Kreykenbohm, L. Barragán, J. Wilms, K. K. Pottschmidt, I. Caballero, P. Kretschmar, F. C, and R. Rothschild, "Study of the many fluorescent lines and the absorption variability in GX 301-2 with XMM-newton," *A&A* **535**, 9 (2011).

7 J. Torrejón, N. Schulz, M. Nowak, and T. Kallman, "A Chandra survey of fluorescence Fe lines in X-ray binaries at high resolution," *ApJ* **715**, 947 (2010).

8 S. Owocki and D. Cohen, "X-ray line profiles from parameterized emission within an accelerating stellar wind," *ApJ* **559**, 1008 (2001).

9 P. Plucinsky, F. Haberl, D. Dewey, A. Beardmore, J. DePasquale, O. Godet, V. Grinberg, E. Miller, A. Pollock, S. Sembay, and R. Smith, "The SMC SNR 1E0102.2-7219 as a calibration standard for x-ray astronomy in the 0.3-2.5 kev bandpass," *SPIE* **7011**, 2 (2008).

10 P. Plucinsky, A. Beardmore, J. DePasquale, D. Dewey, A. Foster, F. Haberl, E. Miller, A. Pollock, J. Posson-Brown, S. Sembay, and R. Smith, "Cross-calibration of the x-ray instruments onboard the Chandra, Suzaku, Swift, and XMM-Newton observatories using the SNR 1E 0102.2-7219," *SPIE* **8443**, 12 (2012).

11 V. Burwitz, F. Haberl, R. Neuhäuser, P. Predehl, J. Trümper, and V. Zavlin, "The thermal radiation of the isolated neutron star RX J1856.5-3754 observed with Chandra and XMM-Newton," *A&A* **399**, 1109 (2003).

12 N. Sartore, A. Tiengo, S. Mereghetti, A. D. Luca, R. Turolla, and F. Haberl, "Spectral monitoring of RX J1856.5-3754 with XMM-Newton. analysis of EPIC-pn data," *A&A* **541**, 66 (2012).

13 M. Ishida, M. Tsujimoto, T. Kohmura, M. Stuhlinger, M. Smith, H. Marshall, M. Guainazzi,

K. Kohei, and T. Ogawa, "Cross spectral calibration of Suzaku, XMM-Newton, and Chandra with PKS 2155-304 as an activity of IACHEC," *PASJ* **63**, 657 (2011).

14 A. Read, S. Rosen, R. Saxton, and J. Ramirez, "A new comprehensive 2d model of the point spread functions of the XMM-Newton EPIC telescopes: spurious source suppression and improved positional accuracy," *A&A* **534**, 34 (2011).

15 S. Mateos, R. Saxton, A. Read, and S.Sembay, "Statistical evaluation of the flux cross-calibration of the XMM-Newton EPIC cameras," *A&A* **496**, 879 (2009).

16 A. Read, M. Guainazzi, and S. Sembay, "Cross-calibration of the XMM-Newton EPIC pn and mos on-axis effective areas using 2XMM sources," *A&A* **564**, 75 (2014).

17 M. Tsujimoto, M. Guainazzi, P. Plucinsky, A. Beardmore, M. Ishida, L. Natalucci, J. Posson-Brown, A. Read, R. Saxton, and N. Shaposhnikov, "Cross-calibration of the X-ray instruments onboard the Chandra, INTEGRAL, RXTE, Suzaku, Swift, and XMM-Newton observatories using G21.5-0.9," *A&A* **525**, 25 (2011).

18 J. Nevalainen, J. David, and M. Guainazzi, "Cross-calibrating X-ray detectors with clusters of galaxies: an IACHEC study," *A&A* **523**, 22 (2010).

19 K. Kettula, J. Nevalainen, and E. Miller, "Cross-calibration of Suzaku/XIS and XMM-Newton/EPIC using galaxy clusters," *A&A* **552**, 47 (2013).

20 G. Schellenberger, T. Reiprich, L. Lovisari, J. Nevalainen, and L. David, "Xmm-newton and Chandra cross-calibration using HIFLUGCS galaxy clusters. Systematic temperature differences and cosmological impact," *A&A* **575**, 30 (2015).

21 K. Mitsuda, N. Yamasaki, K. Shinozaki, Y. Takei, T. Nakagawa, H. Sugita, Y. S. R. Fujimoto, T. Ohashi, Y. Ishisaki, Y. Ezoe, M. Murakami, M. Tashiro, Y. Terada, S. S. Kitamoto,

T. Tamagawa, M. Kawaharada, T. Mihara, R. Kelley, C. Kilbourne, F. S. Porter, P. Shirron, M. DiPirro, D. McCammon, and J.-W. den Herder, "The x-ray microcalorimeter on the NeXT mission," *SPIE* **7011**, E2KM (2008).

22 N. Shaposhnikov, K. Jahoda, C. Markwardt, J. Swank, and T. Strohmayer, "Advances in the RXTE Proportional Counter Array calibration: Nearing the statistical limit," *ApJ* **717**, 59 (2012).

23 C. Wilson-Hodge, M. Cherry, G. Case, W. Baumgartner, E. Beklen, P. N. Bhat, M. Briggs, A. Camero-Arranz, V. Chaplin, V. Connaughton, M. Finger, N. N. Gehrels, J. Greiner, K. Jahoda, P. Jenke, R. Kippen, C. Kouveliotou, H. Krimm, E. Kuulkers, N. Lund, C. Meegan, L. Natalucci, W. Paciesasa, R. Preece, J. Rodi, N. Shaposhnikov, G. Skinner, D. Swartz, A. von Kienlin, R. Diehl, and X.-L. Zhang, "When a standard candle flickers," *ApJ* **727**, 40 (2011).

24 S. Soldi, M. Türler, S. Paltani, H. Aller, M. Aller, G. Burki, M. Chernyakova, A. Lähteenmäki, I. McHardy, E. Robson, R. Staubert, M. Tornikoski, R. Walter, and T. J.-L. Courvoisier, "The multiwavelength variability of 3C 273," *A&A* **488**, 411 (2008).

25 Y. Fukazawa, K. Hiragi, S. Yamazaki, M. Mizuno, K. Hayashi, K. Hayashi, S. Nishino, H. Takahashi, and M. Ohno, "Suzaku view of X-ray spectral variability of the radio galaxy Centaurus A: Partial covering absorber, reflector, and possible jet component," *ApJ* **743**, 124 (2011).

26 T. Kouzu, M. Tashiro, Y. Terada, S. Yamada, A. Bamba, T. Enoto, K. Mori, Y. Fukazawa, and K. Makishima, "Spectral variation of hard X-ray emission from the Crab Nebula with the Suzaku Hard X-ray Detector," *PASJ* **65**, 74 (2013).

27 T. Mineo, G. Cusumano, M. Maccarone, S. Massaglia, E. Massaro, and E. Trussoni, "The hard x-ray emission from the complex SNR MSH 15-52 observed by BeppoSAX," *A&A* **380**, 695 (2001).

28 J. Vink, J. Kaastra, J. Bleeker, and H. Bloemen, "The hard X-ray emission and 44ti emission of Cas A," *AdSpR* **25**, 689 (2000).

29 M. Chernyakova, A. Neronov, T. J.-L. Courvoisier, M. Türler, S. Soldi, V. B. P. Lubiński, R. Walter, K. Page, M. Stuhlinger, R. Staubert, and I. McHardy, "2003-2005 integral and xmm-newton observations of 3c 273," *A&A* **465**, 147 (2007).

30 P. Zhao and L. van Speybroeck, "A new method to model x-ray scattering from random rough surfaces," *SPIE* **4851**, 124 (2003).

31 D. Jerius, T. Geatz, and M. Karovska, "Calibration of Chandra's near on-axis optical performance," *SPIE* **5165**, 433 (2004).

32 T. Gaetz, R. Edgar, D. Jerius, P. Zhao, and R. Smith, "Calibrating the wings of the chandra PSF," *SPIE* **5165**, 411 (2004).

33 Y. Terada, T. Enoto, R. Miyawaki, Y. Ishisaki, T. Dotani, K. Ebisawa, M. Ozaki, Y. Ueda, L. Kuiper, M. Endo, Y. Fukazawa, T. Kamae, M. Kawaharada, M. Kokubun, Y. Kuroda, K. Makishima, K. Masukawa, T. Mizuno, T. Murakami, K. Nakazawa, A. Nakajima, M. Nomach, N. Shibayama, T. Takahashi, H. Takahashi, M. Tashiro, T. Tamagawa, S. Watanabe, M. Yamaguchi, K. Yamaoka, and D. Yonetoku, "In-orbit timing calibration of the Hard X-ray Detector on board Suzaku," *PASJ* **60**, 25 (2008).

34 A. Martin-Carrillo, M. Kirsch, I. Caballero, M. Freyberg, A. Ibarra, E. Kendziorra, U. Lammers, K. Mukerjee, G. Schönherr, M. Stuhlinger, R. Saxton, R. Staubert, S. Suchy, A. Well-

brock, N. Webb, and M. Guainazzi, "The relative and absolute timing accuracy of the EPIC-pn camera on XMM-Newton, from X-ray pulsations of the Crab and other pulsars," *A&A* **545**, 146 (2012).

35 M. Kirsch, U. Briel, D. Burrows, S. Campana, G. Cusumano, K. Ebisawa, M. Freyberg, M. Guainazzi, F. Haberl, K. Jahoda, J. Kaastra, P. Kretschmar, S. Larsson, P. L. K. Mori, P. Plucinsky, A. Pollock, R. Rothschild, S. Sembay, J.Wilms, and M. Yamamoto, "Crab: the standard x-ray candle with all (modern) x-ray satellites," *SPIE* **5898**, 22 (2005).

36 M. Weisskopf, M. Guainazzi, K. Jahoda, N. Shaposhnikov, S. O'Della, V. Zavlin, C. Wilson-Hodge, and R. Elsner, "On calibrations using the Crab Nebula and models of the nebular X-ray emission," *ApJ* **713**, 912 (2010).

37 A. Foster, L. Ji, R. K. R.K. Smith, and N. Brickhouse, "Updated atomic data and calculations for x-ray spectroscopy," *ApJ* **758**, 128 (2012).